Evaluation of Cytochrome P450 Mechanism and Kinetics Using Kinetic Deuterium Isotope Effects†

LeeAnn Higgins, Grace A. Bennett, Miyuki Shimoji, and Jeffrey P. Jones*

Department of Pharmacology and Physiology, University of Rochester, Rochester, New York 14642

Received December 4, 1997; Revised Manuscript Received March 11, 1998

ABSTRACT: In this paper two hypotheses are tested: (i) the active oxygen species is similar in energetics for all cytochrome P450 (CYP) enzymes and (ii) linear free-energy relationships can be used to evaluate the mechanism of the reaction of these enzymes. A series of intramolecular isotope effects were determined and compared for CYPs 1A2, 2B1, 2C9, 2E1, and P450cam. The results indicate that the isotope effects are very similar for each of these isoforms of P450 and that the first hypothesis is likely to be true. Attempts to establish a linear free-energy relationship were only moderately successful: $\log V_{max} = 0.11\sigma^{+}_{p} + 1.73$; $r^2 = 0.588$. It was determined, through the use of intermolecular isotope effects, that the rates of hydrogen atom abstraction are masked. Thus, the second hypothesis is found to be false. This is likely to be a general result for CYP reactions, and linear free-energy relationships can only be used to determine the mechanism under very special circumstances. In all cases, the rate-limiting step should be evaluated with isotope effect experiments before any mechanistic conclusions can be drawn. If the intermolecular isotope effects are found to be masked, no mechanistic conclusion can be drawn from the linear free-energy relationship study.

The cytochrome P450 (CYP)[1] enzymes comprise a superfamily of heme-containing enzymes that consists of more than 300 individual isoforms, and the CYP enzymes are found in plant, bacterial, and mammalian species (*1*). These enzymes function mainly as monooxygenases (*2*). In mammals, they are responsible for the metabolism of certain endogenous as well as exogenous compounds (*3*). Because these enzymes play an important role in xenobiotic metabolism, the abilities to predict reaction rates, identify possible metabolites, and understand CYP mechanisms are important goals. Electronic models have been developed that use computational (*4*, *5*) and chemical (*6*, *7*) approaches for the successful prediction of relative reaction rates and isotope effect profiles for some classes of small compounds.

One of the most important considerations for a potential CYP model is whether the model will apply to relative rate predictions for several (or all) CYP isoforms or for a limited number of isoforms. In this study, we use isotope effect profiles (IEPs) to test the hypothesis that the active oxygen is conserved in multiple CYP isoforms. An IEP consists of isotope effect measurements for a series of structurally related compounds that most nearly approximate intrinsic isotope effects. When intrinsic KIEs are available, comparable trends in IEPs between different systems or different isoforms support similar mechanisms (*6*−*8*).

If the hypothesis that the active oxygen is very similar in multiple CYP isoforms is proven to be true, a single electronic model can be used to describe (the corresponding) multiple P450 enzymes. Linear free-energy relationships are utilized in chemistry and enzymology as a predictive tool and as a probe of the electronic characteristics of the transition state of a reaction. We test here the second hypothesis that LFERs can be used to predict relative rates of metabolism by CYP and to evaluate physical characteristics of CYP reactions. If relative rates of product formation are masked by other steps in an enzymatic cycle, LFERs must be interpreted with caution. Kinetic information, but not mechanistic information, can be deduced, if relative reaction rates are masked. Therefore, it is important to assess whether masking occurs with the substrates chosen for the analysis of a LFER.

Herein, we report IEP results for a series of para-substituted toluenes. The data support the hypothesis of a conserved active oxygen species for multiple CYPs. Our attempts to establish LFERs for a series of para-substituted toluenes were unsuccessful. From isotope effect studies, we conclude that relative reaction rates for para-substituted toluenes in this study are partially masked.

MATERIALS AND METHODS

Chemicals and Reagents. All solvents were purchased from J. T. Baker, Inc. (Phillipsburg, NJ). Chemicals were purchased from Aldrich Chemical Co. (Milwaukee, WI) with the following exceptions: MTBSTFA (+1% *tert*-butyldimethylchlorosilane) was purchased from Regis Technologies,

† This research was supported by the National Institutes of Health, Grants ES06062 and ES09122.

* To whom correspondence should be addressed. Department of Pharmacology and Physiology, Box 711, University of Rochester, 601 Elmwood Avenue, Rochester, NY 14642. Phone: (716) 275-5371. Fax: (716) 244-9283. E-mail: jpj@cyp.medicine.rochester.edu.

[1] Abbreviations: CYP, cytochrome P450; LFER, linear free-energy relationship; IEP, isotope effect profile; KIE, kinetic isotope effect(s); LAD, lithium aluminum deuteride; CH_2Cl_2, dichloromethane; TLC, thin-layer chromatography; NMR, nuclear magnetic resonance; GC−MS, gas chromatography−mass spectroscopy; TK^-, thymidine kinase deficient; KPi, potassium phosphate; Pd, putidaredoxin; PdR, putidaredoxin reductase; *E. coli*, *Escherichia coli*; $NADP^+$, β-nicotinamide adenine dinucleotide phosphate; NADH, β-nicotinamide adenine dinucleotide, reduced; MTBSTFA, *N*-methyl-*N*-(*tert*-butylimethylsilyl)-trifluoroacetamide; HP, Hewlett-Packard; D_0, nondeuterated; D_3, trideuterated; ^{D}V and $^{D}(V/K)$, kinetic deuterium isotope effects on the enzymatic rate constants V_{max} and V/K, respectively.

S0006-2960(97)02986-3 CCC: $15.00
Published on Web 04/23/1998

Inc. (Morton Grove, IL), and potassium phosphate dibasic and monobasic and magnesium sulfate were from EM Science (associate of E. Merck, Darmstadt, Germany). *p*-Chlorotoluene, *p*-methylanisole, and *p*-xylene were purified by distillation before use. *p*-Bromotoluene was crystallized from ethanol, and *p*-tolunitrile was crystallized from benzene: pet ether. Gibco BRL products (Gaithersburg, MD) were used for all cell culture methods. Biochemicals were purchased from Sigma (St. Louis, MO). *p-Xylene*-α, α, α, α′, α′, α′-d_6 (99.8% pure by GC) was purchased from Aldrich Chemical Co.

Synthesis of Compounds. *Para-Substituted Benzyl-α-$^2H_2$ Alcohols.* Methyl 4-bromobenzoate, methyl 4-chlorobenzoate, methyl 4-cyanobenzoate, methyl 4-methylbenzoate, and methyl 4-methoxybenzoate were used as starting materials for the synthesis of the corresponding para-substituted benzyl alcohols according to the following procedure. Lithium aluminum deuteride (1.2 mol) was suspended in ether and cooled to 0 °C in an ice bath while under N_2. The substituted benzoate (1 mol) was dissolved in a small amount of ether and added dropwise to the LAD suspension while keeping the temperature at 0 °C. After the addition, the mixture was stirred at 0 °C for an additional hour, or until complete by TLC (silica gel: 80% hexane, 20% ethyl acetate). The unreacted LAD was decomposed, and the mixture was filtered, dried over $MgSO_4$, and evaporated to dryness. The crude product was purified by recrystallization and/or distillation, and purity was assessed by NMR and GC−MS.

Para-Substituted Toluenes-α,α,α-$^2H_3$. *p*-Bromotoluene, *p*-chlorotoluene, and *p*-methylanisole were synthesized from the corresponding para-substituted benzyl-d_2 alcohols according to the following method. Methane sulfonyl chloride (0.11 mol) was dissolved in a small amount of CH_2Cl_2 and added dropwise to a solution of the para-substituted benzyl-d_2 alcohol (0.10 mol) and triethylamine (0.15 mol) in CH_2Cl_2 that was cooled to −78 °C in a dry ice−acetone bath. The reaction was stirred for another 30 min at −78 °C. Because the mesylates are generally unstable, they were not isolated, and the procedure was continued by adding ice water, separating the layers, and extracting the aqueous layer with CH_2Cl_2. The organic layers were combined, washed with saturated sodium bicarbonate, and dried over $MgSO_4$, and the solvent was removed under reduced pressure. The oil that remained was reconstituted in ether and reduced with LAD using the same procedure as described for the reduction of the benzoates. The products were purified by chromatography (silica gel: 100% CH_2Cl_2), distilled under vacuum using a Kugelrohr, and, when necessary, purified again with a neutral alumina column and 100% hexane to remove any residual benzyl alcohol. Any residual benzyl alcohol was detected by select ion monitoring using GC−MS as described below.

Substituted Toluene-α-$^2H_1$ and -α-$^2H_1$-α′-$^2H_1$. Monodeuterated analogues of *p*-bromotoluene, *p*-chlorotoluene, *p*-methylanisole, and toluene were synthesized by the mesylation of the corresponding nondeuterated benzyl alcohols according to the same procedure described above for the trideuterated compounds, and *p*-xylene-α-$^2H_1$-α′-$^2H_1$ was synthesized with the same method from benzene dimethanol, except that the mole ratio of benzene dimethanol to the other reactants was 1:2.

For *p*-tolunitrile-α-$^2H_1$, the benzyl alcohol was first synthesized by the reduction of *p*-cyanobenzaldehyde using sodium borohydride. For this procedure, the sodium borohydride (0.05 mol) was mixed with about 100 mL of ethanol and stirred under N_2. The aldehyde (0.025 mol) was dissolved in a small amount of ethanol and added dropwise to the $NaBH_4$ solution. The reaction was monitored by TLC (silica gel: 50% ethyl acetate, 50% hexane). After about 1.5 h, the mixture was filtered and the solvent was evaporated. The oil that remained was mixed with water and then extracted with CH_2Cl_2. The organic layer was dried over $MgSO_4$ and evaporated to yield a white solid, which was recrystallized with hexane and assessed for purity by NMR and GC−MS.

Preparation of HepG2-Expressed CYP. Individual CYP isoforms (1A2, 2B1, 2E1, and 2C9) were obtained using the HepG2 vaccinia expression system described previously (*9*). Briefly, the recombinant vaccinia viruses containing cDNAs encoding a single CYP were propagated in human TK^- 143 (human embryoblast) cells, which were then used to infect confluent flasks of hepatoma HepG2 cells (American Type Culture Collection, Rockville, MD). For each isoform, cells were scraped from 50 flasks, pooled, divided into 1-mL aliquots, and stored at −78 °C. Microsomal preparations from crude cell lysates were obtained immediately before use according to the following procedure: aliquots were thawed, mixed with 1 mL of 50 mM KPi buffer pH 7.4, sonicated with a Branson Sonifier Model 450, and centrifuged for 15 min at 300000*g* in a cold (4 °C) Beckman TL-100 ultracentrifuge; pellets were reconstituted with 2 mL of KPi buffer pH 7.4, pooled, and homogenized in a cold room. The total protein concentration of the final enzyme−buffer mixture was typically 3−4 mg mL^{-1} by Bradford assay (*10*) with bovine serum albumin as the standard. The typical low levels of P450 obtained using this expression system were undetectable by CO difference spectra.

Cytochrome P450cam, Putidaredoxin, and Putidaredoxin Reductase. Construction of expression plasmids for P450cam, Pd, and PdR as well as protein expression and purification have been described previously (*11*).

Incubation Conditions and Isolation of Products. All incubations using HepG2-expressed CYP were run for 20 min in a shaking water bath at 37 °C and contained the following: 300−400 μg of protein suspension, depending on the isoform; 10 mM glucose-6-phosphate, 1 mM $NADP^+$, and 1 U glucose-6-phosphate dehydrogenase as an NADPH generating system; and 1400 U catalase in a total volume of 5 mL of 50 mM KPi buffer, pH 7.4, 2 mM $MgCl_2$. For P450cam, the assays were carried out at 37 °C for 20 min in a 1-mL reaction mixture in 50 mM KPi buffer, pH 7.4, 200 mM KCl, 1.5 μM P450cam, 3 μM Pd, 1.5 μM PdR, and 0.3 mM NADH. Reactions were initiated by the addition of 50 μL (HepG2-expressed CYPs) or 10 μL (P450cam) of a substrate solution in CH_3CN, terminated upon addition of 3 mL of CH_2Cl_2, and 10 μL of internal standard in CH_3CN was added, if applicable (see below). Samples were extracted three times with CH_2Cl_2; the organic fractions were pooled, dried with anhydrous $MgSO_4$, and concentrated gently under a stream of N_2 to a volume of approximately 100 μL. After reconstitution with 300 μL (HepG2-expressed CYPs) or 100 μL (P450cam) of CH_3CN, 50 μL of MTB-STFA + 1% *t*-BDMCS was added, and samples were heated overnight at 70 °C.

Enzyme incubations with monodeuterated toluenes and *p*-xylene-α-$^2H_1$-α′-$^2H_1$ were performed in triplicate at a single substrate concentration of 0.25 mM. Determinations of V_{max} and K_m for D_0 or D_3 substrates were made using at least six samples, with six different substrate concentrations in a range between 0.5 and 100 μM, and 10 nmol of the appropriate para-substituted benzyl alcohol as the internal standard. Product formation from D_0 substrates was measured with the corresponding para-substituted benzyl alcohol dideuterated at the benzylic carbon as the internal standard; for D_3 substrates the internal standard was the corresponding nondeuterated benzyl alcohol. Competitive experiments were performed in triplicate with mixtures of D_0 and D_3 substrates, each at a final concentration of 0.25 mM. Linearity studies using low and high concentrations of select D_0 substrates showed linear product formation over 30 min. Two types of controls were run for each substrate with the identical procedure used for the complete samples except that in one case substrate was omitted, and in the other case, $NADP^+$ and the NADPH-generating system or NADH was omitted. Controls for toluene-α-$^2H_1$ showed a small peak at the same retention time as product that originated from the derivatizing agent, which was quantified and subtracted from the observed amount of alcohol product. The kinetic parameters for the metabolism of the substituted toluenes were determined by GC−MS analysis of the M-(dimethylsilyl) derivative of the product benzyl alcohols (see below). Control experiments using a mixture of deuterated and nondeuterated products showed that there was no isotope effect on product workup.

Product Analysis by GC−MS. All samples were analyzed with an HP (Palo Alto, CA) GC/MS 5890/5972 system, equipped with an HP 7673A automatic injector. An HP-1 capillary column (25 m, 0.2-mm ID, 0.5-μm film thickness) was used for product analysis from all substrates except toluene and *p*-xylene, which were analyzed with an HPWax capillary column (30 m, 0.25-mm ID, 0.5-μm film thickness). For the HP-1 column, the injector and detector temperatures were both set at 250 °C; for the HPWax column, the injector and detector temperatures were 230 and 240 °C, respectively. All samples were injected in the splitless mode. Oven conditions for the HP-1 column were 50 °C for 0.5 min, 10 °C/min to 250 °C, and 2 min at 250 °C except when *p*-tolunitrile was used as the substrate, in which case a gradient of 15 °C/min was used. For the HPWax column the oven conditions were 50 °C for 0.5 min, 10 °C/min to 240 °C, and 3 min at 240 °C. The MS was operated at an ionizing voltage of −70 eV and a 20-ms dwell time. Scans of authentic standards of the derivatized benzyl alcohols were used to find peak retention times and to verify products formed from enzyme incubations. Selected ion recording of the M-(dimethylsilyl) ion of products and internal standards was used to determine the amount of metabolism. The ratio of the protio and deuterio products or of the product and internal standard was corrected for ion overlap and percent deuterium incorporation with Brauman's least-squares approach (*12*). Deuterium incorporation of substrates was measured with an HP GC−MS 5890−5970 system with an HP-1 column using the same operating conditions as above except the MS ionizing voltage was adjusted to −10.0 eV.

Scheme 1

$$E + S_H \underset{k_2}{\overset{k_1}{\rightleftharpoons}} [ES_H] \xrightarrow{k_3} [ES_H]_{act} \xrightarrow{k_H} [EP_H] \xrightarrow{k_7} E + P_H$$

$$E + S_D \underset{k_2}{\overset{k_1}{\rightleftharpoons}} [ES_D] \xrightarrow{k_3} [ES_D]_{act} \xrightarrow{k_D} [EP_D] \xrightarrow{k_7} E + P_D$$

$$^DV = \frac{\frac{k_{5H}}{k_{5D}} + \frac{k_{5H}}{k_3} + \frac{k_{5H}}{k_7}}{1 + \frac{k_{5H}}{k_3} + \frac{k_{5H}}{k_7}} \quad (1)$$

$$^D(V/K) = 1 \quad (2)$$

Data Analysis. Kinetic parameters V_{max} and K_m were determined by nonlinear regression using GraphPad Prism v2.01 (San Diego, CA) data analysis software. Kinetic expressions were solved using the program Mathematica (Wolfram Research, Champain, IL).

THEORY

Linear Free-Energy Relationships and KIE. When LFERs are sought, experiments should be performed that definitively answer the following question: *Is the rate of product formation masked (is product formation limited) by a rate-determining step in the catalytic cycle that is not the chemical step of interest?* Fortunately, innovative methods for the investigation of masking in enzymatic systems were developed by Cleland and Northrop (*13*, *14*). With this approach, KIE are measured on the enzymatic parameters V_{max} and V/K. Isotope effects on V_{max} and V/K are expressions for the isotope effects on rates of product formation with the limiting conditions of high and low substrate concentrations, respectively. In this study we report deuterium isotope effects on V_{max} and V/K which are designated ^DV and $^D(V/K)$. The expressions for both ^DV and $^D(V/K)$ contain the rate constant for the isotopically sensitive step, but they differ in the following ways: only ^DV contains the rate constant for the dissociation of product from enzyme, and only $^D(V/K)$ contains the rate constants for the binding of free substrate and enzyme, and dissociation of the first ES complex to free substrate and enzyme. The relative magnitudes of these steps as well as others to the isotopically sensitive step determine the degree to which the intrinsic KIE (the KIE associated solely with the bond breaking step, i.e., k_H/k_D) will be expressed in ^DV or $^D(V/K)$. Therefore, comparisons of ^DV and $^D(V/K)$ isotope effects to an intrinsic KIE can provide information regarding which steps, if any, are involved in masking the relative rates of product formation. These types of studies can reveal if LFERs can be used to make mechanistic conclusions. **It should be noted that even if a linear relationship is seen between the natural log of the rates and the descriptors for a series of compounds, it does not mean that the relative rates are unmasked**.

Intermolecular Isotope Effects. Intermolecular deuterium isotope effects are often used for kinetic and mechanistic studies on enzyme systems. While this type of experiment usually does not provide significant mechanistic information since the intrinsic isotope effect is not observed, it can provide information about the kinetic mechanism. An intermolecular noncompetitive KIE experiment involves the

independent determination of V_{max} and V/K using protonated and isotopically labeled substrates, for example, R_1-CH_3 and R_1-CD_3 (*15*). For the calculation of a KIE, the kinetic constant (V_{max} or V/K) pertaining to the unlabeled substrate is divided by the corresponding constant for the labeled substrate. Scheme 1 shows a potential kinetic mechanism that describes an intermolecular noncompetitive KIE, and eqs 1 and 2 are the expressions for ^{D}V and $^{D}(V/K)$ obtained for this scheme. Substrate (S_H or S_D) combines with enzyme (E) reversibly to form the corresponding ES complex (ES_H or ES_D). (Subscript "H" or "D" signifies the involvement of a compound or a complex in the pathway for the abstraction of hydrogen or deuterium, respectively.) Formation of an "activated" complex ES_H* or ES_D*, from ES_H or ES_D, respectively, is depicted here as an irreversible step that occurs prior to the isotopically sensitive step. This irreversible step is consistent with our understanding of the kinetic mechanism of CYP (*16*, *17*). It is a kinetic representation of a collection of steps that include the following: the first electron reduction ($Fe^{3+} \rightarrow Fe^{2+}$); oxygen binding and reduction; the second electron reduction of oxygen; and the heterolytic cleavage of the peroxy anion, a postulated step which is presumed to be irreversible. Product is formed at the isotopically sensitive step, producing an enzyme−product complex (EP_H or EP_D), which is followed by the dissociation of the corresponding product from the enzyme. Rate constants k_1, k_2, k_3, and k_7 may each actually represent more than one step, and inclusion of these additional steps increases the complexity of the KIE equations but does not modify this analysis. When there is no pathway for alternate product formation, which is typical for most enzymes, the value of ^{D}V depends on the relative magnitudes of k_3 and k_7 to k_{5H}. As the rate constants k_3 and k_7 decrease relative to k_{5H}, ^{D}V becomes masked (see eq 1). $^{D}(V/K)$ for the noncompetitive KIE with the kinetic mechanism shown in Scheme 1, which has no branching pathway from ES_H* or from the corresponding ES_D* position, is completely masked (eq 2).

Scheme 2

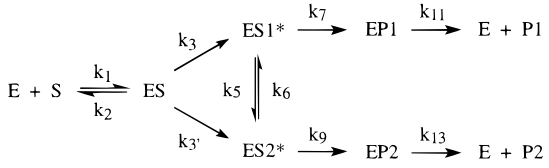

$$^{D}(V/K)_{P1} = \frac{\frac{k_{7H}}{k_{7D}} + \frac{k_{7H}k_6}{k_5k_9} + \frac{k_{7H}}{k_5}}{1 + \frac{k_{7H}k_6}{k_5k_9} + \frac{k_{7H}}{k_5}} \quad (3)$$

$$^{D}V_{P1} = \frac{\frac{k_{7H}}{k_{7D}} + \left[\frac{k_{7H}k_6}{k_5k_9} + \frac{k_{7H}}{k_5}\right] + \left[\frac{2k_3k_{7H}}{k_{13}k_{7D}} + \frac{k_3k_{7H}}{k_{11}k_5} + \frac{k_3k_{7H}}{k_{13}k_5} + \frac{2k_3k_6k_{7H}}{k_{11}k_5k_9}\right]}{1 + \left[\frac{k_{7H}k_6}{k_5k_9} + \frac{k_{7H}}{k_5}\right] + \left[\frac{2_{k3}}{k_{13}} + \frac{k_3k_{7H}}{k_{11}k_5} + \frac{k_3k_{7H}}{k_{13}k_5} + \frac{2k_3k_6k_{7H}}{k_{11}k_5k_9}\right]} \quad (4)$$

While the $^{D}(V/K)$ is completely masked given Scheme 1, a branched pathway has the potential to unmask both ^{D}V and $^{D}(V/K)$ (*18*). This is illustrated using Scheme 2, which represents the formation of two different products (Product 1 = P1, Product 2 = P2) from one substrate, either deuterated or nondeuterated. Metabolism at an alternate, isotopically insensitive step, k_9, is in competition with the isotopically sensitive step, k_7. Rate constants k_1 and k_2 represent substrate binding to and debinding from the enzyme. Rate constants k_3 and k_3' are shown as irreversible steps that represent steps that occur after substrate binding, up to and including oxygen activation. These steps lead to the formation of "activated complexes" (ES1* and ES2*) between the enzyme and the substrate in the relative positions 1 and 2. Rate constants k_3 and k_3' are assumed to be equal for a given substrate. The active oxygen species is stable enough to permit translational and conformational changes of the substrate in the active site of the enzyme (*19*−*21*). Consequently, it is possible for an equilibrium to be established between ES1* and ES2* (see k_5 and k_6). This is the key to unmasking KIE. When deuterium is substituted for hydrogen at the site of metabolism, the rate constant for product formation is reduced. This can be expressed as $k_{7D} < k_{7H}$, where k_{7D} represents the rate constant for oxidation at a deuterated position on a substrate, and k_{7H} represents the rate constant for oxidation at the same position on a nondeuterated analogue of the substrate. Deuterium substitution will cause the concentration of $ES1_D$* to increase relative to the concentration of $ES1_H$* (which is the corresponding enzyme−substrate complex for a nondeuterated substrate) unless $ES1_D$* is in equilibrium with another complex, for example, $ES2_D$*. (The corresponding equilibrium would exist for the nondeuterated substrate as well.) If an alternate pathway does not exist, then $[ES1_D^*] > [ES1_H^*]$, and an isotope effect is masked.

Oxidation at an alternate, unlabeled position on a substrate with the formation of a second product (P2) can unmask a KIE. This is accomplished by the redirection of "excess" $ES1_D$* toward $ES2_D$* which allows $[ES1_D^*] = [ES1_H^*]$, which is necessary for the expression of a maximum, or unmasked, isotope effect. According to the convention of Northrop (*15*), a substrate with a low forward internal commitment to catalysis will branch from ES1 toward ES2 (Scheme 2), and isotope effects on ^{D}V and $^{D}(V/K)$ will be unmasked, depending on the magnitude of the commitment terms. The extent to which $^{D}(V/K)$ is unmasked depends on the relative values of k_5 and k_9 to k_{7H} (eq 3). As the rates of substrate rotation and branching increase relative to the rate of P1 formation, the amount of unmasking increases. The expression for a KIE on ^{D}V for Scheme 2 is quite complex (not shown) but can be simplified to eq 4 with the following two assumptions. If we assume that reduction of oxygen is rate-limiting (see prior discussion) and is significantly smaller than (i) the rotation of substrate in the active site ($k_3 \ll k_5$, k_6) and (ii) the rates of product formation k_{7H} and k_9, the expression for $^{D}V_{P1}$ is simplified to eq 4. If the external reverse commitment to catalysis is small (k_{11}, $k_{13} \gg k_3$), that is, product release is not rate-limiting, then eq 4 reduces to eq 3 ($^{D}V_{P1} = {}^{D}(V/K)_{P1}$).

Cytochrome P450 has the potential to function as an oxidase, whereby molecular oxygen undergoes a four-electron reduction, with the overall formation of two molecules of water (*22*). Formation of the second molecule

of water acts as a branch point leading from the ES complex in Scheme 2 and precludes substrate oxidation. As a consequence, if branching to water is fast relative to product formation, KIE (or rates of product formation) can become unmasked.

Intramolecular Isotope Effects. To obtain better mechanistic information from enzyme kinetic studies, intramolecular KIE can be used. While this type of experimental design cannot be used for all enzymes, in cases where it is appropriate it can be used to provide a closer estimate of the intrinsic isotope effect, since the potential for masking is decreased. For this experiment, a substrate is chosen that contains at least two symmetrical sites, with at least one site, *but not all*, isotopically labeled. An intramolecular KIE is a special case of branched kinetics in that the branch point occurs at the two symmetric sites. Numerous references provide discussions and schemes for intramolecular KIE and their relation to intrinsic KIE (*19*, *23*, *24*).

An intramolecular KIE will always be greater than or equal to an intermolecular KIE. However, it has been shown that even intramolecular KIE can be masked (*19*, *25*, *26*), depending on the choice of substrate. Masking is significantly reduced when substrates are chosen that contain hydrogen and deuterium bonded to the same carbon atom (*26*).

Isotope Effect Profiles. To determine if the mechanisms of two reactions are similar, IEPs are preferred over a single measurement since the trend in isotope effects provides additional information about the energetics of the reaction and makes fortuitous agreement between the two systems unlikely (*27*). An IEP consists of isotope effect measurements in a system (e.g., chemical or enzymatic) using a series of compounds that are structurally related. When intrinsic KIE are available, comparable trends in KIE profiles between different systems argue for similar mechanisms, while different trends are indicative of dissimilar mechanisms. The rationale for this inference is based on the fundamental idea of the Melander−Westheimer principle (*28*, *29*) which is based on the Hammond postulate (*30*). According to the Melander−Westheimer principle, maximum isotope effects will be observed with reactions that have symmetrical reaction coordinates. Mechanisms with nonsymmetrical reaction coordinates will yield smaller isotope effects. From this information it can be inferred that intrinsic KIE that are measured for a series of compounds that differ in some systematic (e.g., chemical or physical) way can serve as a sensitive probe of the energetics of the isotopically sensitive step.

RESULTS AND DISCUSSION

Isotope Effect Profiles with Multiple CYPs. Isotope effect profiles for multiple CYP isoforms were measured in order to test the hypothesis that the active oxygen of multiple CYPs is conserved. The intramolecular isotope effects for six para-substituted toluenes (*p*-X-Ph-CH_2D: X = OCH_3, CH_2D, H, Cl, Br, CN; Ph = phenyl) using expressed CYPs 1A2, 2B1, 2E1, and 2C9 and purified P450cam are listed in Table 1. These experiments were performed with expressed CYP3A4 also, but product formation was too low to accurately measure, most likely because these compounds are poor 3A4 substrates. Isotope effects measured with substrates that contain hydrogen and deuterium bonded to the same carbon atom permit close measurement of the intrinsic isotope effects (see prior discussion of intramolecular isotope effects). Table 1 shows that, for each isoform, the IEPs for the toluenes are practically identical: the values range from 4 to 11, and the magnitudes of the isotope effects have the same rank order. In addition, for each substrate the KIE for all five CYPs are in close agreement, which exemplifies the conserved nature of the active oxygen species.

Table 1: Intramolecular Isotope Effects for Six Para-Substituted Toluenes Using Various CYP Isoforms, Where Isotopic Discrimination Occurs at a Monodeuterated Benzylic Position (i.e., R-CH_2D)[a]

para substituent	2E1	2B1	1A2	2C9	P450cam
OCH_3	4.24 (1)	3.69 (3)	4.64 (4)	4.3 (1)	4.44 (1)
CH_2D[b]	5.45 (5)	6.23 (5)	5.59 (1)	5.9 (1)	6.0 (2)
H	6.1 (1)	7 (1)	6.1 (4)	nd[c]	nd
Cl	6.75 (2)	8.1 (1)	7.06 (2)	6.2 (1)	6.5 (8)
Br	6.75 (3)	8.02 (3)	6.83 (8)	6.9 (2)	8.3 (1)
CN	10.1 (1)	11.9 (3)	10.1 (2)	11.1 (6)	11.6 (5)

[a] CYPs 2E1, 2B1, 1A2, and 2C9 were expressed in HepG2 cells, and P450cam was purified from *E. coli*. Each result is the average of three determinations, and the numbers in parentheses indicate the standard deviation in the last significant digit of the mean isotope effect value. [b] *p*-Xylene-α-$^2H_1$-α′-$^2H_1$ was used as the substrate. [c] Not determined due to low levels of product formation. For each substrate except toluene, a comparison of all the isotope effect values revealed that the means were statistically different from each other at the 0.05 significance level. This is explained by the fact that the standard deviations reflect the precision of the method only and do not take into account systematic and day-to-day errors.

The IEPs presented in this paper provide the first evidence for a common reaction mechanism for aliphatic hydroxylation at the benzylic position in four mammalian CYP isoforms as well as one bacterial isoform. Inclusion of P450cam into our series of IEPs is the first extension of this application to a P450 outside of the Class II P450s. P450cam belongs to Class I, which consists of P450s that interact with two electron-transfer partners. Class II members differ in that they have only one protein as a reducing partner (*31*). The finding that the KIE profile for P450cam is not different from the CYPs that belong to Class II is significant because it indicates that the mechanism of hydrogen atom abstraction is independent of the steps that occur prior to the irreversible formation of an active oxygen species.

Our results agree with other IEP data in the literature for different groups of compounds that are metabolized by CYP. Karki et al. measured isotope effects for a series of *N*,*N*-dimethylanilines using mammalian CYPs 2B1 (purified), 4B1 and 1A2 (expressed), rat liver microsomes, and purified bacterial CYP102 and compared them to KIE in two different chemical systems (*6*). Practically identical IEPs for all of the P450s and the *tert*-butoxyl radical system provide strong evidence for a similar mechanism of *N*-dealkylation, that is, initial hydrogen atom abstraction. Furthermore, the mechanism was conserved among all the CYPs that were tested, which includes both mammalian and bacterial members of the Class II P450s. Isotope effect profiles for various CYPs and for the *tert*-butoxy radical in several small molecules reported by Manchester et al. also support the mechanism of (initial) hydrogen atom abstraction for CYPs (*7*). This abundant amount of data for both mammalian and bacterial isoforms strongly supports a common mechanism for multiple CYPs.

LFER with Para-Substituted Toluenes and CYP2E1. Since the data above support the hypothesis that CYPs act with

Table 2: Kinetic Constants for the Formation of Para-Substituted Benzyl Alcohols from the Corresponding Para-Substituted Toluenes Using Expressed CYP2E1[a]

para substituent	V_{max}[b]	SE[c] V_{max}	V/K[d]	SE V/K	r^2 [e]	n[f]
CN	61.7	0.4	0.014	0.001	1	6
Br	58.5	1.3	0.043	0.005	0.979	12
Cl	50.4	0.8	0.033	0.002	0.998	6
CH_3	58.6	1.2	0.022	0.002	0.990	11
OCH_3	41.0	1.1	0.017	0.002	0.983	11
Br-d_3	54.8	0.8	0.027	0.002	0.997	6
Cl-d_3	31.4	1.0	0.020	0.003	0.991	6
CH_3-d_6[g]	55.7	0.4	0.019	0.001	1	6
OCH_3-d_3	18.0	0.3	0.007	0.001	0.996	6

[a] V_{max} and V/K were determined by nonlinear regression. [b] Units of nM min^{-1}. [c] Standard error of the indicated constant. [d] Units of min^{-1}. [e] Correlation coefficient for the nonlinear regression fit to kinetic data. [f] Number of points used for the determination of kinetic constants V_{max} and V/K. Experiments were performed with nondeuterated or trideuterated (at the benzylic position) substrates, except for *p*-xylene. [g] *p*-Xylene-α, α, α, α′, α′, α′-d_6 was used as the deuterated analogue of *p*-xylene.

similar chemical mechanisms, the next question we addressed was the following: *Can we use linear free-energy relationships (LFER) to predict the relative reaction rates of substituted toluenes?* The first isoform we chose for our kinetic studies was CYP2E1, since this is a low-K_m isoform for small hydrophobic molecules (*32*). The steady-state kinetic constants V_{max} and K_m for benzylic hydroxylation were determined for five para-substituted toluenes (*p*-X-Ph-CH_3: X = OCH_3, CH_3, Cl, Br, CN; Ph = phenyl) using expressed CYP2E1, which displayed typical Michaelis−Menton behavior (Table 2). The choices of para substituents allow for a range of electronic perturbation at the benzylic group; thus we originally explored a LFER with the Hammett constant σ^+_p (*33*). This is an empirically determined physical parameter that indicates the relative degree of electronic perturbation that a substituent imparts in the para position. Hammett constants have been shown in other cases to correlate well with the rates of hydrogen atom abstraction from substituted toluenes (*34*−*36*). We found only poor correlation with V_{max} and σ^+_p (Figure 1, $r^2 = 0.588$) as well as other physical constants (data not shown) and poor correlation with V/K and various parameters. In addition to the poor correlation of V_{max} and σ^+_p, the slope is positive, which is unexpected on the basis of previous correlations of CYP reaction rates with Hammett constants (*37*) as well as rates of H-atom abstraction from toluenes using various oxygen radicals, which yield negative slopes (*34*, *38*). A positive slope indicates that a transition state is stabilized by electron-withdrawing substituents. This would normally be interpreted to mean that the transition state is negatively charged.

We considered two possibilities for the explanation of the poor correlations: (1) electronic parameters do not determine CYP2E1 substrate reactivity; and (2) the kinetic constants (V_{max}, V/K) are masked or partially masked. Both of these possibilities were analyzed with the appropriate methodology and the results are discussed in detail below.

Correlation of Electronic Parameters of Substrates with KIE. First, we addressed the question of whether electronic factors of CYP substrates have any observable effect on the oxidation step. The natural log of the intramolecular KIE for the six toluenes listed in Table 1 is plotted as a function

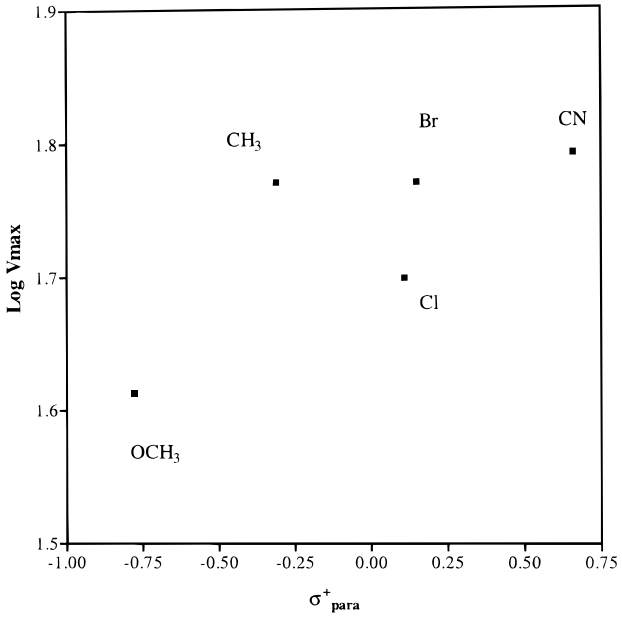

FIGURE 1: Linear free-energy relationship between log V_{max} for benzylic hydroxylation for para-substituted toluenes using expressed CYP2E1 and σ^+_{para}. The para substituent is shown on the plot next to the data point for the corresponding para-substituted toluene. The results from linear regression of the five data points (regression line not shown) are log $V_{max} = 0.11\sigma^+_p + 1.73$; $r^2 = 0.588$.

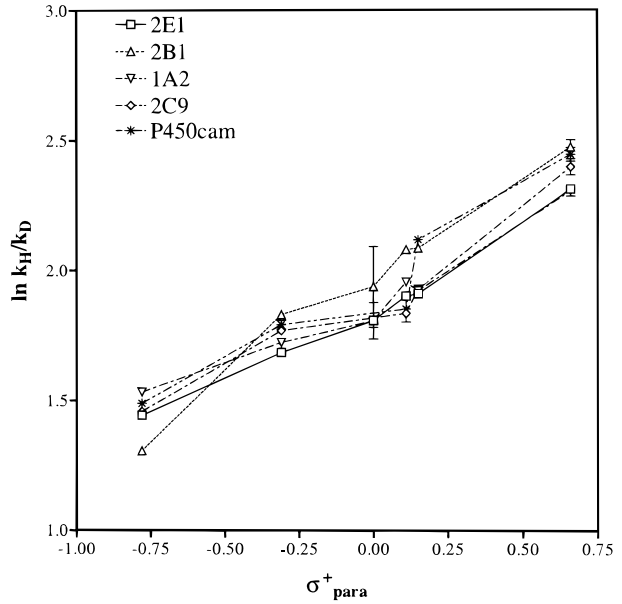

FIGURE 2: Isotope effect trends for multiple CYP isoforms: plot of the natural log of the intramolecular isotope effects for a series of para-substituted toluenes as a function of σ^+_{para} for the corresponding substituents. The substituent and the corresponding σ^+_{para} value are the following (respectively): OCH_3, −0.78; CH_3, 0.31; H, 0; Cl, 0.11; Br, 0.15; CN, 0.66 (*33*). These results show that electronic factors play a role in determining isotope effect magnitudes, and consequently in determining transition-state structure.

of σ^+_p for each para substituent (Figure 2). The results can be explained with a three-center transition-state complex and with Melander and Westheimer's theory for the explanation of small isotope effects (*28*, *29*, *39*). The main concept is that the symmetric stretching vibration can supply isotope-dependent zero-point energy to the transition state, which offsets the isotope-dependent zero-point energy of the ground-state molecules. The isotope-dependent zero-point energy difference in the transition state will be smallest for

Table 3: Comparison of Isotope Effects on Benzyl Alcohol Product Formation for Various Para-Substituted Toluenes Among Three Different Types of Isotope Effect Experiments

CYP	para substituent	intramolecular[a] k_H/k_D	intermolecular noncompetitive[a] ^DV	intermolecular noncompetitive[a] $^D(V/K)$	intermolecular competitive[b] $^D(V/K)$
2E1	Br[c]	6.75 ± 0.03	1.07 ± 0.04	1.58 ± 0.01	2.06 ± 0.07
2E1	CH_3[d]	5.45 ± 0.05	1.05 ± 0.03	1.19 ± 0.01	1.18 ± 0.03
2E1	OCH_3[c]	4.24 ± 0.01	2.3 ± 0.1	2.60 ± 0.01	2.57 ± 0.02
2E1	Cl[c]	6.75 ± 0.02	1.61 ± 0.01	1.62 ± 0.01	3.18 ± 0.62
2B1	Cl[c]	8.06 ± 0.12	nd[e]	nd	3.21 ± 0.02
1A2	Cl[c]	7.06 ± 0.02	nd	nd	2.5 ± 0.1

[a] The numbers after the ± sign are propagated errors. [b] Intermolecular competitive values are expressed as the mean ± standard deviation of three samples. The substrate analogues used for the experiments of intermolecular design were either [c]d_0 and d_3, or [d]d_0 and d_6; only benzylic position(s) were deuterated. [e] Not determined. The intermolecular isotope effects are masked, as compared to the unmasked intramolecular isotope effects, which closely approximate intrinsic values (see Table 1).

an isothermic (symmetric) reaction, giving the largest isotope effect. In our series of substituted toluenes, we propose that the force constant between the benzylic carbon and the abstractable hydrogen is different for each substituent and varies as a function of σ^+_p. The data in Figure 2 support this idea. Furthermore, the CYP primary KIE for octane (*40*) is near the maximal possible value for hydrogen atom abstraction, and according to theory (*28*−*30*), a symmetrical transition state and an isothermic reaction are inferred. Thus, increasingly endothermic reactions relative to octane will yield increasingly smaller intrinsic KIE, and increasingly exothermic reactions will yield increasingly smaller intrinsic KIE; a plot of KIE as a function of σ^+ would be a parabola. The KIE plot shown in Figure 2 demonstrates values that lie on the ascending slope of this curve. We conclude that the transition state is sensitive to electronic effects.

Intermolecular Isotope Effects for Para-Substituted Toluenes. Next, we investigated whether the poor correlation of V_{max} and σ^+_p was caused by the masking of V_{max} by some other (slower) step in the catalytic cycle. Most enzyme-catalyzed reactions contain multiple steps, and it is not uncommon for the masking of reaction rates to occur. This idea is discussed by Eberson (*41*). For CYP reactions, it is generally accepted that the rate-limiting step is the transfer of the second electron from P450 reductase to P450 (16), a step that occurs prior to the formation of product. Consequently, experimentally measured kinetic constants may be partially masked due to the presence of the slow electron-transfer step unless branching to an alternate position is fast enough to unmask the intrinsic value for the kinetic constant under investigation. In summary, information gained from an enzymatic rate measurement is mechanistically meaningless if the rate is not that for the reaction step(s) of interest.

To ascertain if the V_{max} values from Table 2 were masked, intermolecular isotope effects were measured and compared to the corresponding intramolecular KIE from Table 1. Isotope effect experiments of the noncompetitive intermolecular design were performed in order to evaluate the two kinetic constants V_{max} and V/K. Table 3 shows that the observed KIE on both V_{max} and V/K for four of the para-substituted toluenes listed in Tables 1 and 2 range from 1 to 3, while the intramolecular KIE for the corresponding toluenes in 2E1 range from 4 to 8. Since the intermolecular KIE are smaller than the intramolecular KIE, we can conclude that both ^DV and $^D(V/K)$ are masked. The fact that $^DV_{P1} = {}^D(V/K)_{P1}$ values are almost identical supports the fact that the external commitments to catalysis are small (see Scheme 2 and eqs 3 and 4).

The rate eqs 1 and 2 for an intermolecular noncompetitive KIE without branching to alternate product (see Scheme 1) can be used to interpret our results. As the relative ratio of k_{5H} to k_3 and/or k_7 increases, the degree of masking of ^DV increases. An irreversible step preceding the isotopically sensitive step, such as the formation of the active oxygen species, can mask ^DV if it is slow enough. In addition, a slow step following product formation, such as product release, can produce the same effect, depending on its magnitude. For a noncompetitive scheme with no branching from the activated complex ES_H* or ES_D*, $^D(V/K)$ will be equal to 1. Since the $^D(V/K)$ KIE we observed are larger than 1, branching to an alternate pathway (not shown in Scheme 1) may account for the partially unmasked values of 1.2−2.7 that we observed (see eq 3 and relevant discussion). Branching to an alternate oxidation site(s) on the substrate or through the pathway leading to water formation has been shown to unmask isotope effects for various compounds (*17*, *19*, *21*). Branching to water can unmask KIE when there is only a single site of metabolism on a substrate and when metabolism at an alternate site on a substrate is a minor pathway. With most of the substrates used in this study, it is possible that branching to water serves to slightly unmask $^D(V/K)$. Benzylic hydroxylation accounts for 70% or more of the total oxidation of toluene, depending on the source of CYP (*42*, *43*), and ∼95% of *p*-xylene metabolism (*26*, *43*). Ring hydroxylation is energetically less favorable for *p*-bromotoluene, *p*-chlorotoluene, and *p*-tolunitrile, as compared to benzylic hydroxylation. In these cases, since metabolism at the alternate position on the substrate is slower than metabolism at the benzylic group, it cannot fully unmask an isotope effect. Preliminary studies in our lab show that metabolism at the methoxy group of *p*-methylanisole can fully unmask the KIE associated with benzylic hydroxylation (also see Scheme 2 and relevant discussion). The data in Table 3 indicate that at least for *p*-methylanisole and *p*-chlorotoluene the intermolecular isotope effects are slightly unmasked. One likely interpretation is that a small amount of branching to water or aromatic hydroxylation is responsible for this unmasking. Furthermore, since $^D(V/K)$ and ^DV isotope effects are nearly identical, the masking must be due to high internal commitments to catalysis. The distinction between internal and external commitments to catalysis is described by Northrop (*15*).

To confirm the intermolecular noncompetitive KIE data, we measured intermolecular competitive $^D(V/K)$ for the same substrates using CYP2E1 (Table 3). Isotope effects of the intermolecular competitive design are simpler to perform as compared to experiments of noncompetitive design since only one concentration of each substrate (deuterated and nondeuterated) is used. In this type of experiment, both substrates are added to the same incubation mixture at a single (usually equal) concentration, and a competition between the deuterated and nondeuterated compounds is established. Only isotope effects on V/K are measured with experiments of this design (*18*).

The results of the competitively determined $^{D}(V/K)$ for four substituted toluenes are listed in Table 3. The values of 1.2−3.2 indicate that the KIE are masked, when compared to the intramolecular KIE values for the same substrates, which range from 4 to 7. For *p*-xylene and *p*-methylanisole, the $^{D}(V/K)$ KIE determined competitively and noncompetitively are the same. The KIE for *p*-bromotoluene determined by competitive and noncompetitive experiments are 1.5 and 2.1, respectively, and for *p*-chlorotoluene the values are 1.6 and 3.2. The discrepancies in $^{D}(V/K)$ for *p*-bromotoluene and *p*-chlorotoluene can be interpreted in terms of the kinetic constants that define the schemes for the two types of experiments. In experiments of the competitive design only, steps that pertain to debinding of both deuterated and nondeuterated substrates from one (or more) of the ES complexes can potentially unmask (or at least partially unmask) a KIE, depending on the magnitudes of the rate constants for these steps relative to others. The reason for the substrate dependence on the differences in $^{D}(V/K)$ for the toluenes is not known at this time, but it is certain that KIE are masked in both types of experiments.

Competitive KIE experiments were performed for *p*-chlorotoluene using expressed 2B1 and 1A2 to address whether masking of $^{D}(V/K)$ occurs in other CYPs (Table 3). The *V*/*K* isotope effects were 3.1 (2B1) and 2.5 (1A2), as compared to the intramolecular KIE of 8.1 (2B1) and 7.1 (1A2). The results imply that the same degree of masking occurs in all three isoforms (for *p*-chlorotoluene), which suggests that masking may occur by the same mechanism for these isoforms.

Summary. Isotope effect profiles were used to provide evidence that the reacting oxygen species is conserved among a number of P450 enzymes. However, a single electronic descriptor cannot be used to predict relative reaction rates since the chemical step is not rate-limiting. Thus, any electronic model for P450 must take advantage of the fact that branched pathways leading to multiple products are common in P450-mediated reactions. These branched pathways have the effect of unmasking intrinsic reactivity differences which can be described by kinetics analogous to intramolecular isotope effect experiments.

ACKNOWLEDGMENT

The TK$^-$ 143 cells containing recombinant vaccinia virus were generous gifts from Dr. F. Gonzalez. P450cam, Pd, and PdR clones were generous gifts from Dr. J. A. Peterson.

REFERENCES

1. Nelson, D. R., Koymans, L., Kamataki, T., Stegeman, J. J., Feyereisen, R., Waxman, D. J., Waterman, M. R., Gotoh, O., Coon, M. J., Estabrook, R. W., Gunsalus, I. C., and Nebert, D. W. (1996) *Pharmacogenetics 6*, 1−42.
2. Wislocki, P. G., Miwa, G. T., and Lu, A. Y. H. (1980) in *Enzymatic Basis of Detoxification* (Jakoby, W. B., Ed.) pp 135−82, Academic Press, New York.
3. Gonzalez, F. J. (1992) *Trends Pharmacol. Sci. 13*, 346−52.
4. Korzekwa, K. R., Jones, J. P., and Gillette, J. R. (1990) *J. Am. Chem. Soc. 112*, 7042−6.
5. Yin, H., Anders, M. W., Korzekwa, K. R., Higgins, L., Thummel, K. E., Kharasch, E. D., and Jones, J. P. (1995) *Proc. Natl. Acad. Sci. U.S.A. 92*, 11076−80.
6. Karki, S. B., Dinnocenzo, J. P., Jones, J. P., and Korzekwa, K. R. (1995) *J. Am. Chem. Soc. 117*, 3657−64.
7. Manchester, J. I., Dinnocenzo, J. P., Higgins, L., and Jones, J. P. (1997) *J. Am. Chem. Soc. 119*, 5069−70.
8. Hermes, J. D., Roeske, C. A., O'Leary, M. H., and Cleland, W. W. (1982) *Biochemistry 21*, 5106−14.
9. Gonzalez, F. J., Aoyama, T., and Gelboin, H. V. (1991) *Methods Enzymol. 206*, 85−92.
10. Bradford, M. M. (1976) *Anal. Biochem. 72*, 248−54.
11. Shimoji, M., Yin, H., Higgins, L., and Jones, J. P. (1998) *Biochemistry*, in press.
12. Korzekwa, K. R., Howald, W. N., and Trager, W. F. (1990) *Biomed. & Environ. Mass Spectrom. 19*, 211−7.
13. Cleland, W. W. (1975) *Biochemistry 14*, 3220−4.
14. Northrop, D. B. (1975) *Biochemistry 14*, 2644−51.
15. Northrop, D. B. (1982) *Methods Enzymol. 87*, 607−25.
16. White, R. E., and Coon, M. J. (1980) *Annu. Rev. Biochem. 49*, 315−56.
17. Harada, N., Miwa, G. T., Walsh, J. S., and Lu, A. Y. (1984) *J. Biol. Chem. 259*, 3005−10.
18. Northrop, D. B. (1981) *Annu. Rev. Biochem. 50*, 103−31.
19. Jones, J. P., Korzekwa, K. R., Rettie, A. E., and Trager, W. F. (1986) *J. Am. Chem. Soc. 108*, 7074−8.
20. Korzekwa, K. R., Trager, W. F., and Gillette, J. R. (1989) *Biochemistry 28*, 9012−8.
21. Atkins, W. M., and Sligar, S. G. (1987) *J. Am. Chem. Soc. 109*, 3754−60.
22. Gorsky, L. D., Koop, D. R., and Coon, M. J. (1984) *J. Biol. Chem. 259*, 6812−7.
23. Hjelmeland, L. M., Aronow, L., and Trudell, J. R. (1977) *Biochem. Biophys. Res. Commun. 76*, 541−9.
24. Miwa, G. T., Garland, W. A., Hodshon, B. J., Lu, A. Y., and Northrop, D. B. (1980) *J. Biol. Chem. 255*, 6049−54.
25. Dinnocenzo, J. P., Karki, S. B., and Jones, J. P. (1993) *J. Am. Chem. Soc. 115*, 7111−6.
26. Iyer, K. R., Jones, J. P., Darbyshire, J. F., and Trager, W. F. (1997) *Biochemistry 36*, 7136−43.
27. Karki, S. B., and Dinnocenzo, J. P. (1995) *Xenobiotica 25*, 711−24.
28. Melander, L. (1960) *Isotope Effects on Reaction Rates*, Ronald Press, New York.
29. Westheimer, F. H. (1961) *Chem. Rev. 61*, 265−73.
30. Hammond, G. S. (1955) *J. Am. Chem. Soc. 77*, 334−40.
31. Peterson, J. A., and Graham-Lorence, S. E. (1995) in *Cytochrome P450: Structure, Mechanism, and Biochemistry* (Ortiz de Montellano, P. R., Ed.) pp 151−80, Plenum Press, New York.
32. Guengerich, F. P., Kim, D.-H., and Iwasaki, M. (1991) *Chem. Res. Toxicol. 4*, 168−79.
33. Hansch, C., and Leo, A. (1979) *Substituent Constants for Correlation Analysis in Chemistry and Biology*, John Wiley & Sons, New York.
34. Kim, S. S., Koo, H. M., and Choi, S. Y. (1985) *Tetrahedron Lett. 26*, 891−4.
35. Sakurai, H., and Hosomi, A. (1967) *J. Am. Chem. Soc. 89*, 458−60.
36. Heberger, K. (1994) *J. Phys. Org. Chem. 7*, 244−50.
37. White, R. E., and McCarthy, M. B. (1986) *Arch. Biochem. Biophys. 246*, 19−32.
38. Zavitsas, A. A., and Pinto, J. (1972) *J. Am. Chem. Soc. 94*, 7390−6.
39. Kresge, A. J. (1977) in *Isotope Effects on Enzyme-Catalyzed Reactions* (Cleland, W. W., O'Leary, M. H., and Northrop, D. B., Eds.) pp 37−63, University Park Press, Baltimore.
40. Jones, J. P., Rettie, A. E., and Trager, W. F. (1990) *J. Med. Chem. 33*, 1242−6.
41. Eberson, L. (1990) *Acta Chem. Scand. 44*, 733−40.
42. Hanzlik, R. P., and Ling, K.-H. J. (1990) *J. Org. Chem. 55*, 3992−7.
43. Tassaneeyakul, W., Birkett, D. J., Edwards, J. W., Veronese, M. E., Tassaneeyakul, W., Tukey, R. H., and Miners, J. O. (1996) *J. Pharmacol. Exp. Ther. 276*, 101−8.

BI9729864